Top Catal (2008) 50:133–144
DOI 10.1007/s11244-008-9113-0

ORIGINAL PAPER

Synthesis of TiO_2 Thin Films: Relationship Between Preparation Conditions and Nanostructure

C. Ampelli · Rosalba Passalacqua · Siglinda Perathoner · Gabriele Centi · Dangsheng S. Su · Gisela Weinberg

Published online: 9 August 2008

Abstract The influence of the synthesis conditions (pH, HF concentration, procedure of application of the voltage) during the anodization of Ti foils to produce TiO_2 thin films characterized by an ordered arrays of 1D nanostructures (nanorods, nanotubes) is discussed. Different types of 1D nanostructures could be obtained by changing the procedure of synthesis, as shown by field emission scanning electron microscopy images. The analysis of the current versus time curves during the procedure of synthesis provides indications on the sequence of processes occurring during the synthesis. It is also suggested that different growing mechanisms occur depending on the preparation, leading in turn to the different type of nanostructures observed. The relevance of this preparation method is related to the analysis of the relationship for oxide materials between nano-architecture and reactivity and gives the opportunity to prepare materials with an intermediate degree of complexity between model and applied catalysts.

Presented at the Robert Karl Grasselli Foundation Symposium on Advances in Selective Heterogeneous Oxidation Catalysis, Irsee, Germany 7–10 June 2007.

C. Ampelli · R. Passalacqua · S. Perathoner (✉) · G. Centi
Department of Industrial Chemistry and Engineering of Materials and ELCASS, University of Messina and INSTM UdR Messina, Salita Sperone 31, 98166 Messina, Italy
e-mail: perathon@unime.it

G. Centi
e-mail: centi@unime.it

D. S. Su · G. Weinberg
Department of Inorganic Chemistry and ELCASS, Fritz Haber Institute of the Max Planck Society, Faradayweg 4-6, 14195 Berlin, Germany

Keywords Titania · Anodization · Nanotubes · Nanorods · Nanostructured thin film

1 Introduction

Metal-oxides are catalysts used in a wide range of applications, from acid-base to redox reactions and photocatalytic processes, due to their multiple functional properties [1]. The control of the catalyst multi-functionality requires the ability to control their nano-architecture, e.g., the 3D spatial arrangement around the sites of adsorption [2]. The surrounding around the active site plays an important role, because it orients or assists the coordination of the reactants, may induce sterical constrains on the transition state, and influences short-range transport (nano-scale level). This is well demonstrated in the case of anchored metal organic complexes, but much less attention has been given in the evaluation of the same aspects in the case of oxide catalysts [1, 3].

Only limited studies on the control of the nano-structure and -architecture of oxides are available. Most of the oxide catalysts do not have a well defined 3D structure (both on short and long-range), being composed of irregularly-shaped nano-crystals. These materials are polycrystalline, and show several nano-interfaces, which stabilize micro-strains, oxygen vacancies or metal ions in unusual coordination states. A 3D environment for adsorption/transformation may significantly modify the adsorption of reactants and stabilization of transition state complexes, a well-known concept for enzymes, but typically not considered for solid catalysts.

Significant advances have been made recently on nano-fabrication techniques to synthesize metal-oxides. An example of such catalysts is given by ordered arrays of

vertically aligned 1D nanostructures prepared by anodic oxidation [4–6]. The technique has a relatively low cost and is potentially scalable, while other techniques, such as electron beam lithography show limitations for scale-up and may be mainly used to prepare ordered patterns of metal nanoparticles [7–9].

These materials prepared by anodic oxidation represent an interesting opportunity for the development of novel catalysts [10] to be used to bridge the material gap in catalysis [11]. Nanostructuring the surface in terms of ordered arrays of nanotubes allows, for example, to prepare a dense array of nano-reactors, opening interesting perspectives for a better control of the 3D architectures of active sites and to integrate homogeneous, heterogeneous and bio-catalysis in a surface-confined nano-drop [10].

Other possible creative ways exists in which control of the surface nano-architecture allows to prepare novel catalysts. For example, let us consider a surface characterized by an array of vertically aligned nanorods. It may be expected that the properties of the apical part of the nanorods are different from those of the walls (similarly to what is known for carbon nanotubes) and reasonably different from the properties of the oxide layer at the bottom of the nanorods. These different properties may be used to prepare multi-functional catalysts with specific 3D organization. It is known, for example, that the walls of titania nanorods can be preferentially capped by organics, such as oleic acid or amines [12]. The adsorbed species may act as surface ligands to anchor complexes and in general to selectively change the hydrophilic characteristics of these materials. It is also known that the TiO_2 nanorods act as inorganic stabilizers similar to surfactant molecules, for example allowing stabilization of colloidal noble metal nanoparticles [13]. During depositing of noble metal particles, differentiation between preferential deposition on the apical, basal and wall sides of nanorods can be thus observed.

Ordered arrays of 1D nanostructures offer thus new possibilities for the design of catalysts as well as to bridge the gap between homogeneous and heterogeneous catalysis. These materials offer also a new 3D design of the surface, which can be relevant to stabilize supported enzymes and microorganisms, providing new opportunities to prepare heterogeneized biocatalysts. From the modeling point of view, these metal-oxide thin films constituted by ordered arrays of 1D nanorods or nanotubes could represent an intermediate level of complexity between well-ordered metal-oxide films used for theoretical modeling in surface science studies and real catalysts.

There are thus several motivations to investigate the possible use of these nano-organized oxide thin films for catalytic applications, but the first issue is a better understanding on the control of the nano-architecture of these materials. In fact, notwithstanding the fast growing literature on the subject, most of the developed materials are not suited for uses as catalysts, being developed for other applications [10]. In addition, often results on a systematic control of the surface nanostructure are missing. For example, several studies on the preparation of titania nanotubes has been published [14–25], but often a more specific correlation between the nanostructure and synthesis parameters is missing.

We will present here the preparation of titania thin films by controlled anodic oxidation. These films are characterized by an ordered array of vertically aligned 1D nanostructures and we will analyze how the nanostructure of the titania thin film depends on some synthesis parameters. We used titania (TiO_2) for this investigation, because it is (i) an interesting support in a number of catalytic applications, (ii) a catalyst itself in some applications (Claus reaction, for example), and (iii) shows a high photocatalytic activity.

Different methods have been proposed to synthesize 1D-like titania nanostructures [10]. We focused our attention on the preparation of ordered nanostructured thin films of titania by anodic oxidation of titanium foils, because this method is easy to be scaled-up, is low costly and allows to obtain ordered patterns of 1D nanostructures. The essence of the method may be described as a reconstruction of a thin titania layer (formed initially by oxidation of a titanium foil) which occurs under the application of a differential potential which creates also strong local electrical fields at the surface. By controlling this parameter, different types of 1D titania nanostructures could be prepared. In previous studies, we discussed the characteristics and photocurrent properties of ordered helical nanocoil arrays [26, 27] and how these materials could represent a good model system in studies bridging the material gap between ordered crystals used in surface studies and real catalysts [11]. We will instead discuss here the influence of the preparation procedure on different characteristics of titania thin films which could be tailored. On the other hand, different ordered nanostructures could be of great interest for catalytic studies, because in this way it is possible to change the catalytic nano-architecture while maintaining very similar the preparation method. As far as we know there are no other examples of preparation methods with these characteristics.

2 Experimental

TNT films were prepared by anodizing titanium foils (Alfa Aesar, 30 × 40 mm) of thickness 2.0 mm and purity 99.2%. The foils were first sonicated in distilled water, and then in isopropyl alcohol for 10 min each. Then they were dried in air.

Anodic oxidation was made in a stirred electrochemical cell working at room temperature which cell geometry was described earlier [11]. The well stirred cell operates at room temperature and atmospheric pressure, has an electrolyte volume of 33 mL and a 10 mm distance between the two electrodes. The Ti foil is immersed for about 90% in depth and is connected to an electrical wire through a metallic connector. A Pt wire was used as cathode.

An Autolab PGSTAT30 potenziostat/galvanostat in a two electrode set-up was used to apply different constant anodizing voltages 10, 15, and 20 V for times typically of 45 min. Typical anodization procedure adopted was to immerse the Ti foil in the electrolyte and rapidly raise the potential to the final value (in the 10–20 V range), maintaining constant this value for all the time of the experiment. After immerging the Ti foil, the current passing through the circuit was monitored. In a second procedure, the initial voltage (10 V) was maintained for 20 min and then a linear ramp was applied up to the final voltage (23 V range) which was then maintained constant for 2 min. The increase of voltage rate was changed from 0.2 to 1 V/min.

The electrolyte consisted of 0.3–0.7 wt% HF in double distilled water. The pH of the solution was 0 or 4.0. In the latter case, the pH was increased by addition of a concentrated NH_4OH aqueous solution. AA and XRF were used to check the purity of the solutions, and to analyze the amount of Ti dissolved in solution after anodization, but in general Ti ions were not detected in the electrolyte after the anodization procedure. The samples were cleaned with deionized water at the end of the anodization process and then dried overnight. Further calcination at 450 °C in air do not change the observed nano-structure.

The structural and morphological characterization of the titania thin films was made by a Scanning Electron Microscop Hitachi S4800 with FEG (Field Emission Gun) (FESEM). About 5 kV were typically used to record the images. The chemical composition was determined by EDX.

3 Results

The process of anodization used to prepare the nanostructured titania thin films may be summarized as follows, by analogy with the formation of porous alumina by anodization [28, 29] which was studied in more detail, even if indications on the reaction mechanism have been suggested also for titania thin films produced by anodization [30–32].

When the Ti foil, after the preliminary cleaning treatment, is immersed in the electrolyte for the anodization process, a fast surface oxidation occurs with formation of a thin TiO_2 layer. This process may be monitored by a fast decrease of the current, being the TiO_2 layer not conductive. Due to the presence of an aqueous solution of HF as electrolyte, the solubilization of Ti^{4+} ions and/or of small TiO_2 particles starts simultaneously with the formation of the oxide layer. These processes lead to the formation of holes which locally modify the electrical field and induces from one-side the acceleration of the process of dissolution, due to field-enhanced effects, and from the other side the oriented growing of 1D structures (nanotubes, nanorods, etc.). All these processes are strongly influenced by the reaction conditions, which in turn determine the characteristics of the different nanostructures. However, little attention was given in literature to understand the relationship between conditions of synthesis and type of ordered nanostructures produced. This understanding is of importance in general terms, but also specifically for studies aimed to identify the use of these materials for catalysis.

3.1 Effect of Voltage During Anodization

The voltage has a relevant role on the nanostructure of titania films. Reported in Fig. 1 are the current versus time curves observed for three samples during anodization at constant voltage (10, 15, and 20 V) and pH of 4.0. The main graph shows the initial region (up to 6 min) for the three curves obtained at the three different potentials, while in the inset the full curve observed for the sample prepared at constant voltage of 15 V is shown. As indicated above, the initial fast current decrease is due to the oxidation of the Ti foil.

The increase of the anodization voltage causes a lowering of the initial slope (during the first 20 s), e.g., an apparent decrease in the rate of oxidation (Fig. 1a). The decrease of current is associated to a decrease of conductivity related to the formation on an oxide non-conductive barrier over the Ti foil. However, we indicate as apparent this behavior, because two concomitant effects are present. In fact, after this initial fast current decrease, a minimum is present and then the current increases. This second effect is associated to the formation of holes in the oxide layer with a consequent increase on conductibility. The two processes (formation of the oxide layer and formation of the holes in this layer) occur simultaneously. It is reasonable to consider that the rate of formation of the oxide layer increases with the anodization voltage. However, the increase of anodization voltage causes an increase in the rate of formation of holes in the oxide layer. The result is that the initial slope decreases on increasing the anodization voltage, but not because the rate of formation of the oxide layer decreases. This result is confirmed from the observation that the oxide layer thickness increases with the anodization voltage. Note, that the current which is reached after

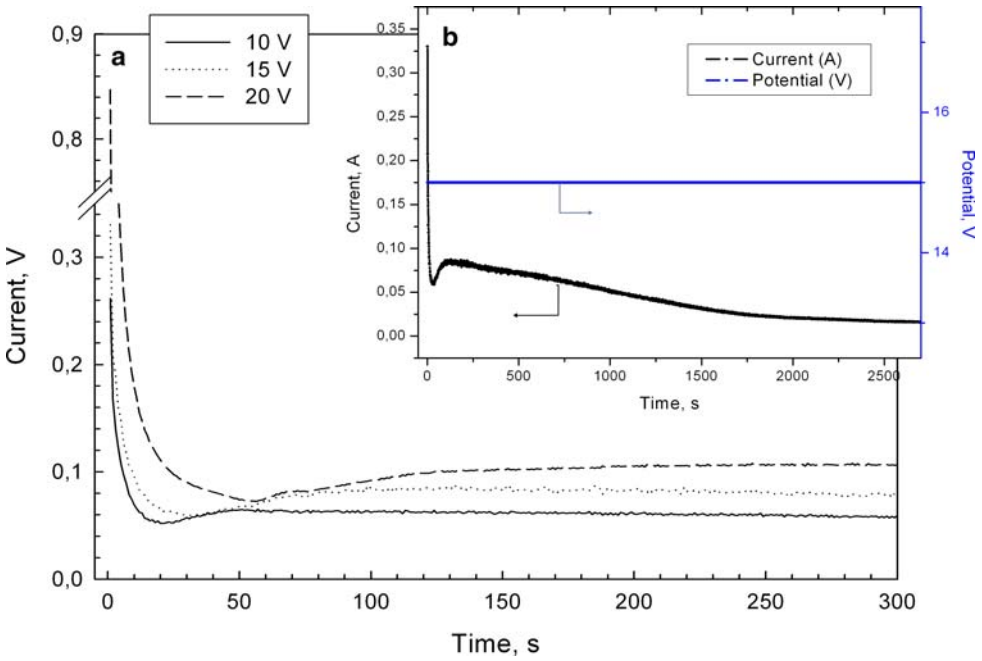

Fig. 1 Current versus time during the anodic oxidation of a Ti foil. Main graph: expansion for the initial region (first 6 min) for samples prepared at constant anodization voltage (10, 15, and 20 V). Inset: full current curves for the sample prepared at 15 V. Electrolyte: [HF] = 0.5 wt%, pH = 4.0

about 150–200 s increases with the increase of anodization voltage. This is consistent with above observations.

For longer times of anodization (after about 200 s) the current further decreases due to the increase of the thickness of the nanostructured titania layer (Fig. 1b). The overall process may be thus schematically divided in three steps: initially (about first 20 s) the dominant effect is the formation of an oxide layer, although already starts the partial dissolution of this layer with formation of holes. Between approximately 20 and 200 s the dominant effect is the reconstruction of this oxide layer with formation of 1D nanostructures and finally for times higher than 200 s the dominant process is the growth of these 1D nanostructures (nano-tubes, -rods, etc.).

The influence of the anodization voltage on the nanostructure of titania films is shown in Fig. 2 which reports FESEM images at lower and higher magnification of three samples prepared by anodization at constant voltage and pH of 4.0 (conditions as in Fig. 1). Images a1–a2 refer to the sample prepared at bias voltage of 10 V, images b1–b2 at voltage 15 V and images c1–c2 at voltage of 20 V. The images at lower magnification (a1, b1, c1) show that large uniform nanostructured areas could be obtained and that TiO_2 particles are not present on the surface. The surface of the Ti foils used was not perfectly flat and thus a moon-like surface could be observed with relatively large depressions (some microns). However, an uniform nanostructure (ordered array of titania nanotubes) is present in all these regions. No preferential orientations at grain boundaries could be observed. A closer inspection at the regions, where these depressions are present, indicate that the growing direction of the nanotubes is always perpendicular to the local plane of the support (see inset of Fig. 2a1). The colour of these nanostructured thin films is blue-violet and the UV–visible diffuse reflectance spectra show the presence of the typical interferences fringes for thin oxide films associated to film thicknesses between 300 and 500 nm. The color is uniform in all the Ti foil, except in the region close to the electrolyte–air interface. This part is characterized by a gray color and FESEM images indicate the absence of a defined ordered nanostructure.

Therefore, an ordered growing process of TiO_2 nanostructures is observed and not simple the dissolution of Ti^{4+} and/or TiO_2 nanoparticles and their random aggregation. Note that EDX analysis and GAXRD (Glancing angle X-ray diffraction) results [27], in agreement with literature data, indicate the presence of only titania in these nanostructures, with no or minimal contamination by fluoride ions. Note also that Ti ions have not been detected in the electrolyte after the anodization, pointing out that the process of dissolution and growing of nanostructures is only local, due to the electrical field, and do not involve long-range transport to the solution. It is thus confined to an electrical field above the surface of the titanium foil.

The images at higher resolution in Fig. 2 (a2, b2, c2) evidence in all cases the presence of an ordered array of nanotubes. Increasing the anodization voltage the mean diameter of these nanotubes increases from about 30 nm (10 V) to 50 nm (15 V), and 70 nm (20 V). The diameter of nanotubes is rather uniform. Wall thickness of these nanotubes is few nanometers and slightly increases on increasing the anodization voltage. The density of packing

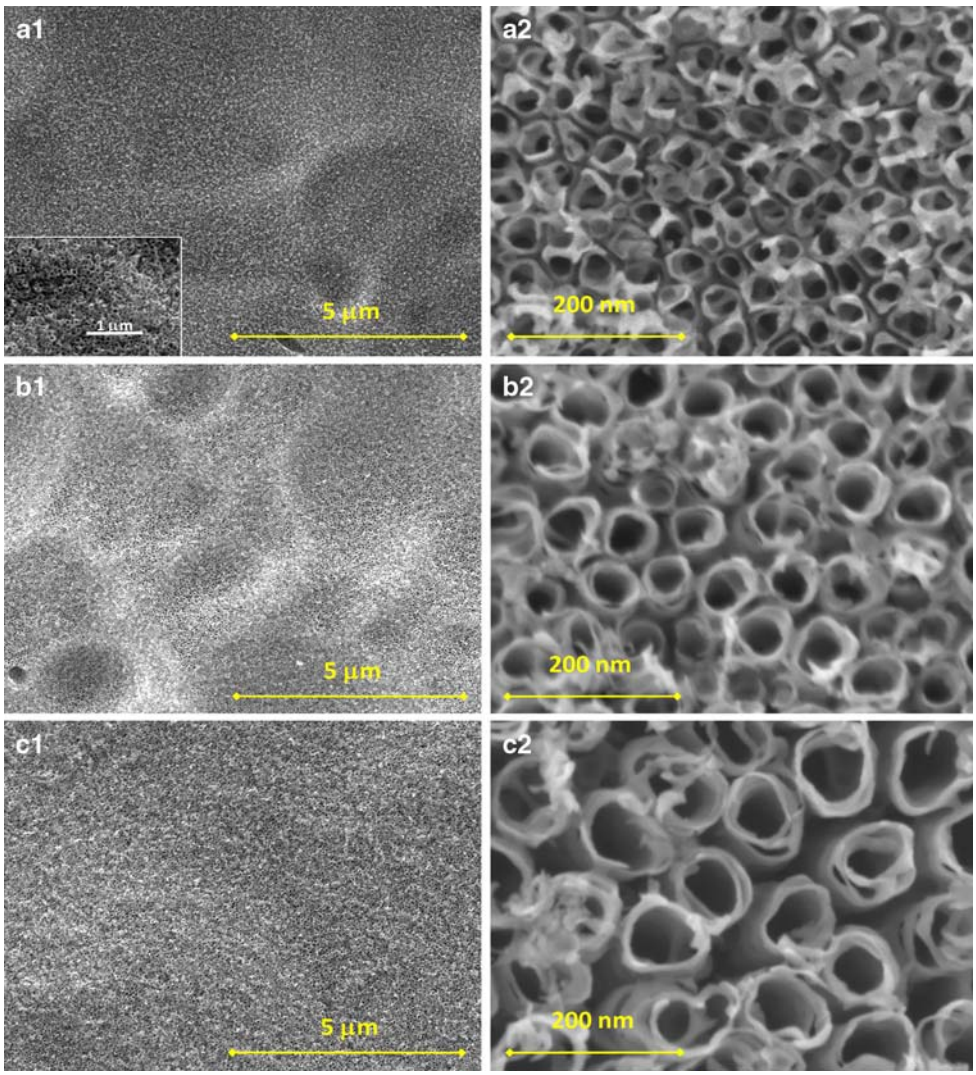

Fig. 2 FESEM images at low and high magnifications of the sample synthesized as in Fig. 1: (a1,a2) 10 V, (b1,b2) 15 V, and (c1,c2) 20 V

also slightly increases. The ratio between the area occupied by the nanotubes and the total area increases from 0.30 (10 V) to 0.35 (15 V), and 0.36 (20 V), in agreement with the discussion above in relation to Fig. 1a. A closer inspection reveals that these nanotubes are separated each other, with reduced contact points between them (see Fig. 2c2). The depth of these nanotubes is about 200–300 nm and rather uniform for the various nanotubes.

3.2 Effect of pH and HF Concentration

Figure 3 reports the current versus time curve for a sample prepared at a constant voltage of 15 V, an HF concentration in the electrolyte of 0.5 wt%, and a pH of zero, e.g., the same conditions as for the sample b in Figs. 1 and 2, but at lower electrolyte pH. This graph should be compared with the trends observed in the inset of Fig. 1 (similar conditions, but pH 4.0 instead of zero). The main observation is that the current decreases not immediately, but initially remains relatively high and only after about 100 s decreases and follows a trend similar to that discussed for the former samples.

Figure 4a shows the low magnification FESEM image of this sample. An uniform nanostructure is present and separate TiO_2 particles could not be detected, similarly to what discussed for the samples in Figs. 1 and 2. Figure 4b shows the nanostructure observed after short anodization time (about 5 min). It is a honeycomb-like nanostructure, quite different from that observed in Fig. 2, due to the presence of compact walls between the holes. After longer time of anodization (Fig. 4c) the nanostructure shows closer analogies to the samples shown in Fig. 2, although the specific morphological characteristics of the nanotubes are slightly different. In particular, the nanotubes in Fig. 2 seem to derive from the rolling of a tape (see Fig. 2c2), while in this case (Fig. 4c) the nanostructure is closer to that of hollow cylinders. It may be noted also that the packing is denser and there are also closer contacts between the nanotubes. Wall thickness is also higher, ranging from 10 to 20 nm, and thus at least twice with

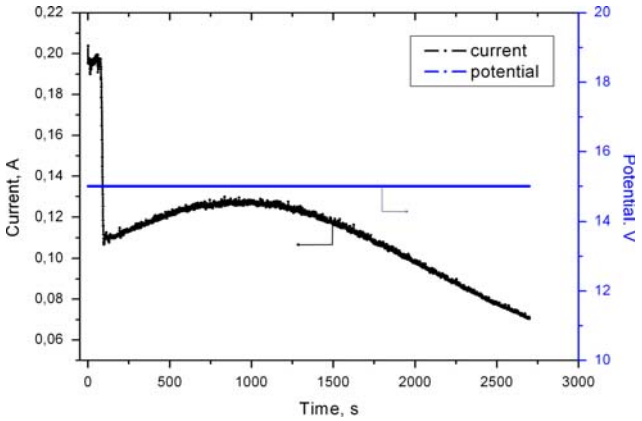

Fig. 3 Potential applied and current observed during the anodic oxidation of Ti foil. Electrolyte: [HF] = 0.5 wt%, pH = 0. Potential kept constant at 15 V during the experiments

respect to those observed at higher pH (Fig. 2). Figure 4c shows also a part of a titania film which was detached from the substrate and allows a better evidence of the nanostructure and the presence of ring-shaped moulds. At lower pH, the overall process is similar to that observed at pH = 4.0, but probably changes the relative rates of the field-enhanced solubilization of Ti^{4+} ions versus TiO_2 nanoparticles with a change in the morphology of the produced nanostructured titania thin film.

Figure 5 shows the cross-section of this titania thin film which indicates the presence of an uniform nanostructured layer with thickness of around 250–300 nm and holes crossing the entire thickness of the oxide film. Note that the Ti interface, on the top of which the nanotubes are grown, is relatively flat. This indicates that a process of depth dissolution is absent, e.g., with the creation of holes, such as that present during alumina anodization.

In the inset the nanostructure of a portion of the oxide film is better highlighted. The bottom of the film is formed by TiO_2 and has a thickness of around 10 nm. The tubes growth is vertically oriented over this bottom layer.

Changing the concentration of HF, quite different results were instead obtained. Reported in Fig. 6 are the FESEM images of samples prepared in analogs conditions as those reported in Fig. 4, but using a 0.3 wt% (Fig. 6a) or a 0.7 wt% (Fig. 6b) concentration of HF (instead of 0.5 wt%—Fig. 4). The nanostructure is quite different and could be described as an ordered array of vertically aligned rods. A closer look evidences that these rods derives from the gluing of nearly round-shaped TiO_2 nanoparticles with mean diameter around 140–160 nm. Their gluing forms mainly vertical rods with mean diameter of 170 or 140 nm for samples prepared at [HF] = 0.3 and 0.7wt%, respectively. The diameter of these nanorods is relatively uniform, indicating again the presence of a mechanism of ordered growth, although some irregular particles are present on the surface. It can be noted, however, that they also derive from the gluing of TiO_2 nanoparticles (see arrows in the expansions of the images). On the surface of the oxide layer, where the electrical field is weaker, a random growth leads to irregularly shaped particles, while closer to the bottom of the oxide layer, where the field is stronger, a regular vertical growth is observed. The density of packing of these nanostructures is higher with respect to that of the nanotubes (around 0.8–0.9 versus 0.3–0.4 for nanotubes) as far as the density of the film.

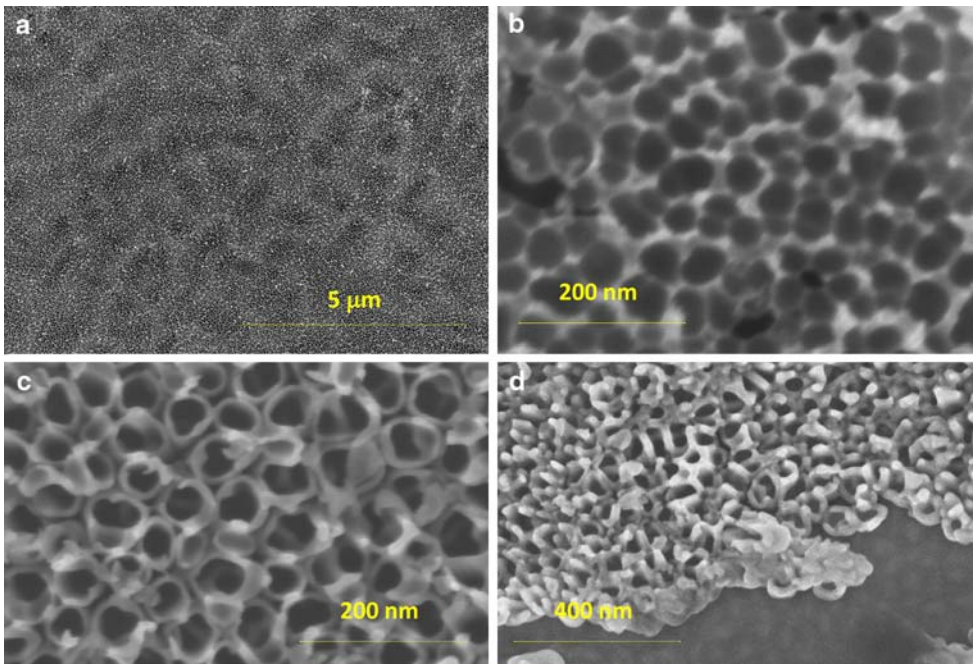

Fig. 4 FESEM images of a sample prepared as in Fig. 3: (**a**) low magnification image, (**b**, **c**) sample after 2 and 45 min of anodization, (**d**) image of a part which was partially detached from the substrate

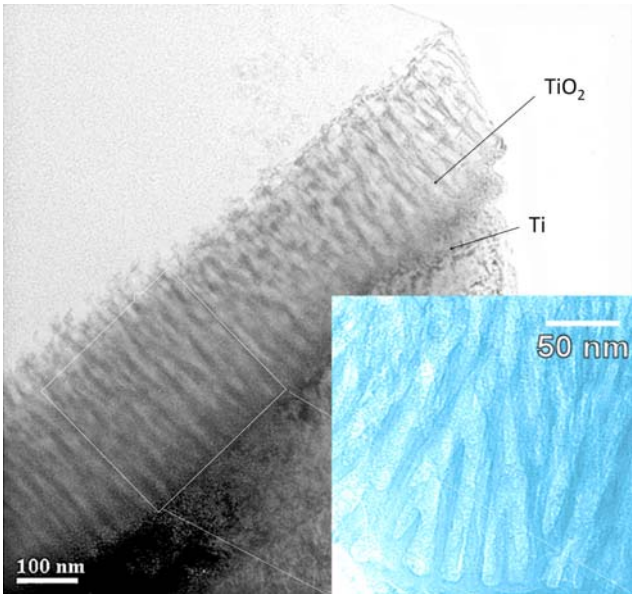

Fig. 5 FESEM cross-section image of the sample prepared as in Fig. 3. In the inset view of a detail of the nanotubes (the image was colored to better evidence the details)

A significant influence of the mechanism of formation of titania nanostructures is observed by changing the concentration of HF. As discussed above, the formation of titania nanotubes derives from the presence of various competitive processes which in turn are influenced from the electrical field. The current versus time curves during the anodization process (Fig. 7) are also quite different from those observed for nanotubes (Figs. 1 and 3). After an initial fast decrease associated to the formation of the oxide layer, the current

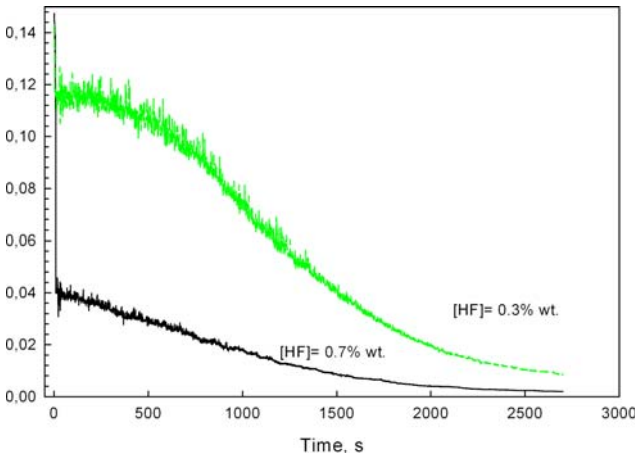

Fig. 7 Current versus time curves obtained during the synthesis of samples of Fig. 6 by anodic oxidation

remains relatively high and decreases then with a slow rate. In comparison with Figs. 1 and 3, the increase of the current after the initial fast decrease is absent. As discussed before, the current increase is associated to the mechanism of creation of holes leading to the formation of nanotubes. Changing the HF concentration, the electrical double layer and the electrical field at the solid–liquid interface also change. Therefore, the relative rates of the processes discussed above (field-enhanced oxidation and dissolution, oriented grow) also modify. This determines a change of the morphology of the 1D titania nanostructures which are obtained. Note also that the current is lower in the case of the sample prepared at HF concentration of 0.7%, in agreement with a lower density of the titania film.

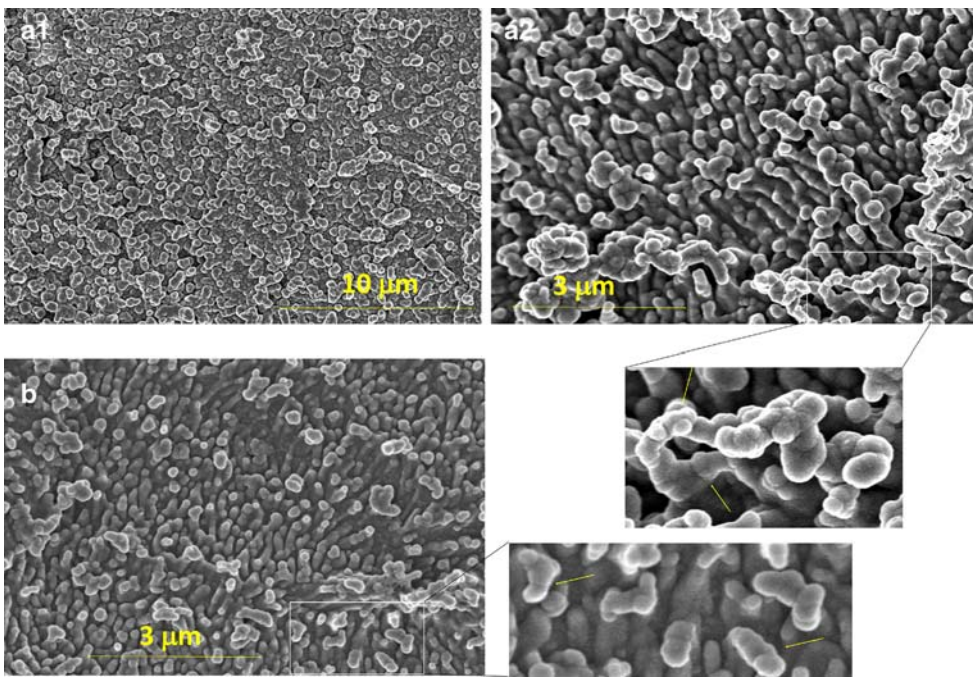

Fig. 6 FESEM images of sample produced by Ti foil anodization at pH = 0 and HF concentration of 0.3 wt% (a1,a2) and 0.7 wt% (**b**)

3.3 Effect of Voltage at pH = 0

The effect of a constant voltage applied during anodization at pH = 0 and [HF] = 0.5 wt%, e.g., synthesis conditions as in Figs. 3 and 4 apart from the voltage, on the nature of the nanostructure of the titania layer is shown in Figs. 8 and 9 for anodization voltages of 20 and 10 V, respectively.

At the higher voltage (20 V, Fig. 8) a nanostructure similar to that observed for the sample of Fig. 4 is present. However, the clear presence of irregularly-shaped TiO_2 nanocrystals (dimensions from around 50 to over 200 nm) over the first nanotube-like layer could be clearly observed (Fig. 8a, b). The mean diameter of the nanotubes is similar in the two cases (around 50 nm for 15 V—Fig. 4—and around 55–60 nm for 20 V—Fig. 8d) and also the packing density, although a slightly larger distribution of nanotubes diameters is observed for the sample prepared at the higher voltage.

In the image of the sample obtained after short time of anodization (5 min, Fig. 8c) it is possible to observe some features which suggest that at pH = 0 the mechanism of

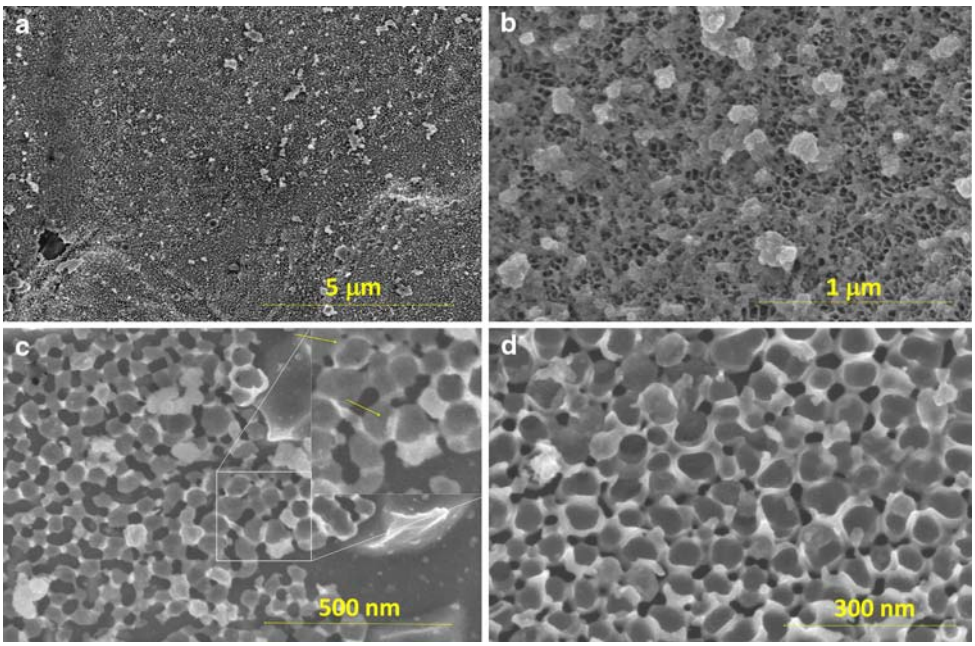

Fig. 8 FESEM images of samples obtained by anodization at [HF] = 0.5 wt%, pH = 0 and constant anodization voltage of 20 V: (**a**, **b**, **d**) low and higher magnification images of sample after 45 min; (**c**) after 5 min

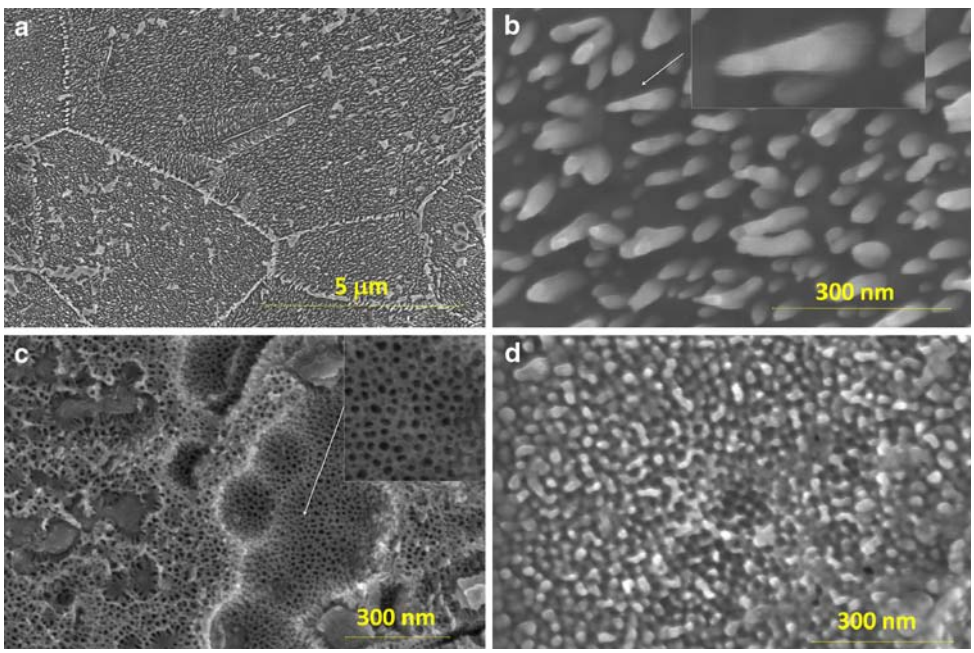

Fig. 9 FESEM images of samples obtained by anodization at [HF] = 0.5 wt%, pH = 0 and constant anodization voltage of 10 V: (**a**, **b**) low and higher magnification images of the sample after 45 min anodization; (**c**) region at the interface between air and the electrolyte; (**d**) region between the less-dense nanorod array (**b**) and the sponge-like region (**c**)

formation of nanotubes could be different from that observed at pH = 4 (Fig. 4). In fact, Fig. 8c, recorded at the perimeter of a nanostructured titania film, shows clearly that (i) holes forms at the grain boundaries between the round-shaped TiO_2 grains with mean diameter similar to that of the final titania nanotubes, and (ii) that walls start to growth at this perimeter edge of TiO_2 grains. During further anodization walls grow and a fully developed array of nanotubes is present after 45 min (Fig. 8d). Therefore, although the final morphological characteristics of the nanostructured titania film are similar at pH = 0 and pH = 4, the growth mechanism of the nanotubes is probably different, explaining the different morphologies of the titania nanotubes and the differences observed in the current versus time curves.

At lower anodization voltage (10 V, Fig. 9) different morphologies for the titania film could be instead observed. Already at low magnification (Fig. 9a) the differences are evident. Relatively large areas (several microns) covered uniformly by nanorods (which concentrate at the titanium grain boundaries) could be observed. The nanorods (Fig. 9b) show a much lower packing degree with respect to those observed in Fig. 6. Although a concentration at Ti grain boundaries is observed, suggesting a preferential growing at defects, the relatively uniform growth over the entire surface indicates a mechanism of formation not linked to defect sites, because an ordered distribution of defects over the surface is not reasonable. The mean diameter of these nanorods (around 15–20 nm) is different from that of the main TiO_2 grains formed at higher anodization voltage and at which perimeter the walls grow to form finally the TiO_2 nanotubes (Fig. 8c). Therefore, when the growth mechanism of 1D nanostructures becomes dominant already at short anodization times, only small and quite well dispersed TiO_2 patches form. Further TiO_2 nanoparticles formed by oxidation are fast solubilized and glued over the top of the growing nanorods due to the different local electrical field. Note in the inset of Fig. 9b that these nanorods have not a cylindrical shape, but a larger diameter at the bottom (around 20–30 nm) and a smaller diameter at the top (about 10 nm). It may be also observed in the top part of the nanorods (inset in Fig. 9b) that the shape and growing do not derive from a continuous growing process, but from the gluing of TiO_2 round-shaped particles with mean diameter of about 10 nm.

Although the largest part of the Ti foil is characterized by a structure as that shown in Fig. 9a, the region at the interface between air and electrolyte (to realize the electrical connection the foils are immersed only for about 90% of the surface in the electrolyte, as reported in the experimental part) shows a more irregular morphology (Fig. 9c), with the presence of a nanotube-like (or honeycomb-like) structure similar to that discussed with reference to Fig. 4b. The mean diameter of these holes, however, is smaller, being around 5–10 nm. A region characterized from a dense array of small nanorods (Fig. 9d) at the interface between the less-dense nanorod array (Fig. 9b) and the sponge-like region (Fig. 9c) could be also observed. Note, that in general all samples prepared by anodization show a different nanostructure and color at the interface between the electrolyte and air, even if this aspect was not discussed above for reasons of conciseness. In general terms, the oxide film in this interface region is more irregular, presenting often the absence of well ordered nanostructures, and moreover it is thicker.

It is reasonable to attribute the different morphology in the interface region to a higher dissolved oxygen concentration in the electrolyte which leads to a higher rate of oxygen diffusion across the electrical double layer, forming thus a thicker oxide layer, typically not showing a well defined nanostructure. This is consistent with the results of Yae et al. [33] and Ogawa et al. [34] who observed that the etching of n-Si wafers in HF solution is enhanced by oxygen dissolved in the solution. Similarly, we may consider that the higher oxygen concentration in solution at the electrolyte–air interface favors a higher rate of etching of the titanium foil which leads to the ticker titania layer, although characterized by a less-ordered growing. This fact points out that by a finer check of the concentration of oxygen in HF solution, a better control of the nature/density of the growth of 1D TiO_2 nanostructures could be obtained.

3.4 Effect of Voltage Ramp

All samples discussed above were prepared at a constant voltage in the 10–20 V range. A different procedure was also adopted maintaining initially the sample at a potential of 10 V for 20 min and then increasing the potential to 23 V (which was then kept constant for 2 min) at a different voltage increase rate in the 0.2–1.0 V/min range. Figure 10 shows the FESEM images at low and higher resolution of the samples prepared at a voltage increase rate of 0.216 V/min (a1, a2), 0.5 V/min (b1, b2) and 1.0 V/min (c1, c2).

In the three cases a nanostructure close to that shown by the sample in Fig. 9 was observed, but an even less-dense array could be noted. In Fig. 9 the density of nanorods was about 350 nanorods per μm^2, while in Fig. 10(a1) about 100 per μm^2. The density of nanorods slightly increases on increasing the voltage rate, but the mean length of the nanorods decreases from about 300 to 100 nm or less. The shape of the nanorods is cylindrical in both cases, with a diameter of around 10–20 nm. At the highest voltage increase rate (Fig. 10 c1, c2) the shape of the nanorods instead changes to an arrow-like shape. In all three

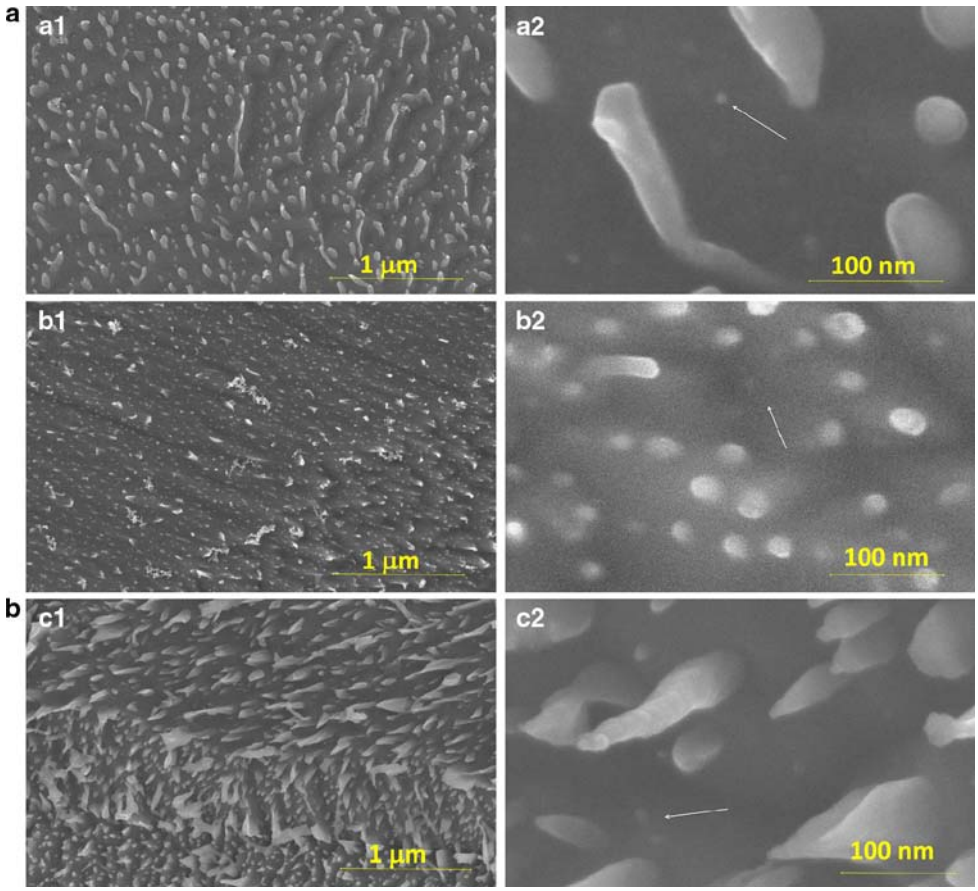

Fig. 10 FESEM images of samples obtained by anodization at [HF] = 0.5 wt%, pH = 0 and the following procedure for anodization: 10 V for 20 min, then increase at different rate up to 23 V which is maintained constant for further 2 min. Rate of voltage increase: 0.216 V/min (a1, a2), 0.5 V/min (b1, b2), 1 V/min (c1, c2)

samples, together with well-developed nanorods, a new incipient nanorod formation could be observed (see arrows in the figures). Note that the diameter of these just forming nanorods is typically smaller with respect to those of the well-developed nanorods. There is thus a first nucleation centre which first increases in diameter and then in depth. The growing mechanism appears thus slightly different from those discussed before. Note also that the images in Figs. 2 and 4 show the presence of 1D nanostructures with uniform depth, while this is clearly not present in the case of samples showed in Fig. 10.

4 Discussion and Conclusions

The first general observation is that by anodic oxidation of titanium foils, it is possible to obtain by the same method, but changing the synthesis parameters, ordered arrays of vertically aligned 1D TiO_2 nanostructures: nanorods and nanotubes. As far as we know, there are no other methods which allow to obtain similar types of materials. The results showed that under appropriate reaction conditions relatively large and uniform areas could be produced, without the presence of irregularly-shaped TiO_2 nanocrystals. This synthesis method thus offers unique characteristics to prepare catalytic thin films with a regular and ordered nano-architecture. Many other methods for TiO_2 nanotubes or nanorods preparation are reported [5, 10, 35–37], although they do not allow to convert them to an ordered array, besides sometimes to other problems related to contamination. For example, under strong basic conditions in an autoclave it is possible to convert TiO_2 nanoparticles to nanotubes, but the purification to remove all Na contamination is difficult and it is well-known that Na traces could affect significantly the catalytic reactivity.

Materials prepared by anodic oxidation offer thus interesting opportunities as model systems to bridge the gap between surface science and applied catalysis. In fact, the thin film could be used in a number of spectroscopic and surface science studies to investigate the relationship between nanostructure and reactivity. It offers an intermediate degree of complexity between well-ordered clean crystals used in surface science studies and real catalysts. Goodman [38], over 10 years ago, pointed out that, despite the successes in modeling catalysts with single crystals, a clear need to develop models with higher levels of complexity is necessary. It should be also observed that ordered arrays of 1D nanostructures as those produced by anodic oxidation are often characterized from minimal interfaces between the 1D nanostructures itself. Onishi and Iwasawa

[39] clearly pointed out the role of the interfacial chemistry on metal-oxides on the reactivity. Worth noting is also that for metal nanoparticles supported on metal-oxides, the interface between the two phases plays a relevant catalytic role [40].

We have shown here that many synthesis parameters affect the nanostructure of the final material, but under strict control of the preparation conditions, a good reproducibility is possible. A relatively large variety of nano-architectures, in terms of shape of 1D nanostructures and their packing density, could be obtained. EDX analysis reveals that no contamination is present in the samples, apart from traces of F ions which could be removed by appropriate washing. Therefore, using the same methodology it is possible to obtain a range of nanostructured titania thin films and use them for studies aimed to investigate structure–activity and selectivity relationships. To note that it has been reported that also other types of similar nanostructured oxide films could be produced by controlled anodization (for example, CuO and WO_3) [41, 42]. Anodization of aluminum can also produce an ordered nanostructure [43], although resembling more a nanomembrane (array of nanoholes) than nanostructures as those shown in the case of titanium anodization. Note, however, that highly ordered WO_3/TiO_2 composite nanotubes have been prepared using anodic alumina as template [44]. It is thus possible to combine the features of these different materials to prepare in principle novel catalysts. It may be concluded that the anodization of metallic films to produce a nanostructured thin oxide film characterized by an ordered array of 1D nanostructure is a general methodology of great potential interest to produce materials for catalytic applications.

The main issue of the method for catalytic application is how to pass from flat surfaces (Ti foils) to more complex and higher surface area geometries (3D macro-structured catalysts). In fact, for an oxide thin film of about 1micron thickness, the amount of oxide is about 0.2 mg/cm^2 of Ti foil (about 0.1 mg for each side of the foil). To increase the oxide weight to amounts relevant for catalytic testing it is thus necessary to increase the geometrical surface area of the surface on which the nanostructured oxide film forms. A first simple option is to use thin metal foils. In this work, we reported homogeneous results obtained for relatively thick Ti foils (2 mm), but we used successfully thin foils (0.025 mm) as well. By stacking multiple foils it is possible to create a monolith-type reactor. For thin foils of thickness 0.025 mm, a stack formed from at least 200 overlapped foils could be created per centimetre of reactor height. In this case, the total amount of oxide per cubic centimetre of reactor reaches a value of 40–50 mg. Note as reference, that in a typical commercial monolith used for treatment of car exhaust emissions, the amount of washcoat (oxide layer where the catalytic components are deposited) is about 150–200 mg/cm^3. Due to the low amount of oxide, it was not possible to measure directly the surface area, but considering for example a geometrical area determined from an array of hollow cylinders of diameter 50 nm and an height one micron, with a packing density of 0.35 as in the images of Fig. 2, the total surface area (assuming no microporosity) is about 8–10 times higher than the geometrical area of the plane on which grows these nanotubes, e.g., about 80–100 m^2/g of oxide layer.

The other possible approach to create a 3D macro-structured catalysts is to first deposit a thin coating of titanium (by sputtering, electrochemical deposition or other methods) on a macro-shaped support (a conductive carbon foam, for example), and then create the nanostructured titania layer by anodization of the titanium thin layer. Alternatively, a Ti foam could be used directly for the anodization.

There are thus different possible approaches to develop higher total surface area catalysts by anodization. Although further research is needed to verify the preferable routes, the above discussion shows that, in principle, the use of the anodization route to develop novel catalysts is possible. In fact, as pointed out in the introduction, besides to the advantage of developing catalysts with a well defined hierarchically organized structure, the presence of an ordered array of 1D nanostructures offers some interesting characteristics, such as the possibility to (i) nanostructure the surface in the form of catalytic nano-reactors, for the integration of homogeneous, heterogeneous, and bio-catalysis, (ii) control the 3D architectures of active sites, and (iii) heterogeneize liquid phase reactions creating surface-confined nano-drops [10, 11].

In conclusion, this contribution offers an indication on how to prepare titania thin films characterized by ordered arrays of nanorods or nanotubes, and control their characteristics. These materials could be interesting to bridge the material and complexity gap in catalysis, but also to develop novel catalysts, even if further research is needed to exploit this potential possibility. Nevertheless, the results could open the door to more specific studies on this issue, because the preparation of this kind of materials is still not common in the field of catalysis.

Acknowledgments This work was realized in the frame of the collaboration with the EU Network of Excellence IDECAT (Integrated Design of Catalytic Nanomaterials for a Sustainable Production), contract NMP3-CT-2005-011730) and of ELCASS (European Laboratory for Catalysis and Surface Science). G. Centi, S. Perathoner and R. Passalacqua also thanks the EU project NATAMA (NMP3-CT-2006-032583) for the financial support.

References

1. Centi G, Cavani F, Trifirò F (2001) In: Twigg MV, Spencer MS (eds) Selective oxidation by heterogeneous catalysis. Recent developments. Fundamental and applied catalysis. Kluwer/Plenum Publishing Corporation, New York
2. Centi G, Perathoner S (1999) Curr Opin in Solid State Mater Sci 4:74
3. Centi G, Perathoner S (2003) Catal Today 79–80C:3
4. Bavykin DV, Friedrich JM, Walsh FC (2006) Advanced materials, vol 18. Wiley-VCH, Weinheim, p 2807
5. Mor GK, Varghese OK, Paulose M, Shankar K, Grimes CA (2006) Solar Energy Mater Solar Cells 90:2011
6. Varghese OK, Grimes CA (2003) J Nanosci Nanotechnol 3:277
7. Somorjai GA, ACS Symposium series (2005), 890 (Nanotechnology and the Environment), 210. Am Chem Soc
8. Wong K, Johansson S, Kasemo B (1996) Faraday Discuss 105:237
9. Caruso RA (2003) Top Curr Chem 226:91
10. Centi G, Perathoner S (2007) Nano-architecture and reactivity of titania catalytic materials. Quasi-1D nanostructures. In: Spivey JJ (ed) Catalysis, vol 19. Royal Society of Chemistry Publishers, Cambridge, p 367
11. Centi G, Passalacqua R, Perathoner S, Su DS, Weinberg G, Schlögl R (2007) Phys Chem Chem Phys 9:4930
12. Cozzoli PD, Kornowski A, Weller H (2003) JACS 125:14539
13. Cozzoli PD, Comparelli R, Fanizza E, Curri ML, Agostiano A, Laub D (2004) JACS 126:3868
14. Mor GK, Varghese OK, Paulose M, Mukherjee N, Grimes CA (2003) J Mater Res 18:2588
15. Varghese KO, Grimes CA (2003) J Nanosci Nanotechnol 3:277
16. Varghese OK, Gong D, Paulose M, Keat KG, Dickey EC, Grimes CA (2003) Adv Mater 15:624
17. Wahl A, Augustynski J (1998) J Phys Chem B 102:7820
18. Adachi M, Murata Y, Harada M, Yoshikawa S (2000) Chem Lett 8:942
19. Uchida S, Chiba R, Tomiha M, Masaki N, Shirai M (2002) Electrochemistry 70:418
20. Macak JM, Tsuchiya H, Schuki P (2005) Angew Chem 44:2100
21. Albu SP, Ghicov A, Macak JM, Hahn R, Schmuki P (2007) Nano Lett 7:1286
22. Macak JM, Zlamal M, Krysa J, Schmuki P (2007) Small 3:300
23. Ghicov A, Aldabergenova S, Tsuchyia H, Schmuki P (2006) Angew Chem Int Ed 45:6993
24. Zhao J, Wang X, Sun T, Li L (2005) Nanotechnology 16:2450
25. Macak JM, Albu SP, Schmuki P (2007) Phys Status Solidi RRL 1:181
26. Perathoner S, Passalacqua R, Centi G, Su DS, Weinberg G (2007) Stud Surf Sci Catal, (TOCAT5, Science and Technology in Catalysis 2006, Kodansha/Elsevier) 172:437
27. Perathoner S, Passalacqua R, Centi G, Su DS, Weinberg G (2007) Catal Today 122(1–2):3
28. Patermarakis G (1998) J Elec Anal Chem 447:25
29. Diggle JW, Downie TC, Goulding CW (1969) Chem Rev 69:365
30. Varghese OK, Gong DW, Paulose M, Grimes CA, Dickey EC (2003) J Mater Res 18:156
31. Gong D, Grimes CA, Varghese OK, Hu W, Singh RS, Chen Z, Dickey EC (2001) J Mater Res 16:3331
32. Zhao J, Wang X, Sun T, Li L (2005) Nanotechnology 16:2450
33. Yae S, Kawamoto Y, Tanaka H, Fukumuro N, Matsuda H (2003) Electrochem Comm 5:632
34. Ogawa H, Ishikawa K, Suzuki MT, Hayami Y, Fujimura S (1995) Jpn J Appl Phys 34 (Part 1):732
35. Grimes CA (2007) J Mater Chem 17:1451
36. Bavykin DV, Friedrich JM, Walsh FC (2006) Adv Mater 18:2807
37. Chen X, Mao SS (2006) J Nanosci Nanotechnol 6:906
38. Goodman DW (1995) Chem Rev 95:523
39. Onishi H, Iwasawa Y (1997) In: Roberts MW (ed) Interfacial science. Blackwell, Oxford, p 57
40. Guczi L, Paszti Z, Frey K, Beck A, Peto G, Daroczy CS (2006) Top Catal 39:137
41. Wu X, Bai H, Zhang J, Chen F, Shi G (2005) J Phys Chem B 109:22836
42. Hahn R, Macak JM, Schmuki P (2007) Electrochem Comm 9:947
43. Masuda H (2005) Highly ordered nanohole arrays in anodic porous alumina. In: Wehrspohn RB (eds) Ordered porous nanostructures and applications. Springer, New York, p.37
44. Cheng L, Zhang X, Liu B, Wang H, Li Y, Huang Y, Du Z (2005) Nanotechnology 16:1341